Journal of Applied Electrochemistry **31**: 1301–1306, 2001.

Hydrogen concentration in water from an Alkali–Ion–Water electrolyzer having a platinum-electroplated titanium electrode

KENJI KIKUCHI[1]*, HIROKO TAKEDA[1], BEATRICE RABOLT[1], TAKUJI OKAYA[1], ZEMPACHI OGUMI[2], YASUHIRO SAIHARA[3] and HIROYUKI NOGUCHI[3]
[1]*Department of Materials Science, University of Shiga Prefecture, 2500 Hassaka, Hikone, Shiga 522-8533, Japan*
[2]*Graduate School of Engineering, Kyoto University, Kyoto 606-01, Japan*
[3]*Matsushita Electric Works, Ltd., Research & Development Center, Home Appliances Co. Kadoma, Kadoma, Osaka 571-8686, Japan*
*(*author for correspondence, e-mail: kikuchik@mat.usp.ac.jp)*

Received 10 November 2001; accepted in revised form 18 September 2001

Key words: current density, hydrogen concentration, supersaturation, water electrolysis

Abstract

The supersaturated concentration of hydrogen in electrolyzed water obtained from a flow-type electrolytic cell was studied under various electrolysis conditions. The degree of supersaturation was found to decrease as the solution supply rate to the cell increased. The ratio of observed hydrogen concentration to the theoretical hydrogen concentration obtained from the electrochemical equivalent, as calculated from the transfer of charge in the cell, was found to increase with the solution supply rate. The concentration of hydrogen in solution has a maximum at a current density of approximately 0.3 A dm^{-2}. This maximum was found to be independent of the flow rate, indicating that the hydrogen concentration is related to both the diffusion of dissolved hydrogen from the electrode surface to the bulk solution and hydrogen bubble growth.

1. Introduction

The electrolyzed water obtained from the cathode chamber of an electrolytic cell is supersaturated with hydrogen. Many electrochemical studies have been conducted concerning the characterization of hydrogen evolution, and various mass transfer models have been proposed to explain gas bubble formation behavior during the water electrolysis [1–11]. Such studies have targeted cathodic reduction of water in alkaline aqueous solutions. Bendrich et al. [12] estimated the mass transfer at the hydrogen gas-evolving electrode, taking two effects into account; microconvective and macroconvective mass transfer. In their study, they assumed that the microconvective effect due to bubble growth was the dominant factor affecting the mass transfer of hydrogen under conditions of high current density and low flow velocity, whereas macroconvective mass transfer, or hydrodynamic flow along the electrode, is the primary factor at high electrolyte velocity and low current density. Shibata [13, 14] reported on the supersaturation of hydrogen in a solution near a gas-evolving electrode, as determined by a current-interruption method, and proposed a relationship between the degree of supersaturation at the electrode surface and current density.

Electrolyzed water from the cathode chamber of electrolyzers has recently been shown to have a range of beneficial effects on health when ingested, including the anti-oxidative property of dissolved hydrogen gas in ethyldocosahexanoeate solution [15–17]. Previous investigations have involved the examination of electrolytic solutions only the vicinity of the electrode surface, and the properties of electrolyzed solutions after electrolysis remain unclear. In the present study, the supersaturation of hydrogen in electrolytic solution is characterized at low current density and low solution velocity along the electrode surface, and the relationship between the velocity and concentration of hydrogen is examined.

2. Experimental

All chemicals used were of reagent grade. The size of the platinum powder used ranged from 0.2 to 2 μm, and water was purified by ultra-filtration of deionized and distillated water before preparing solutions. The electrolysis device consisted of a tank, two pumps, a 25-nm pore filter (Millipore), an electrolytic cell, and Teflon pipes. A schematic of the electrolytic cell used in the present study is shown in Figure 1. The electrolytic cell had two electrodes and a membrane diaphragm separating the cathodic chamber from the anodic chamber. The electrodes were 0.2 cm from the membrane, and the

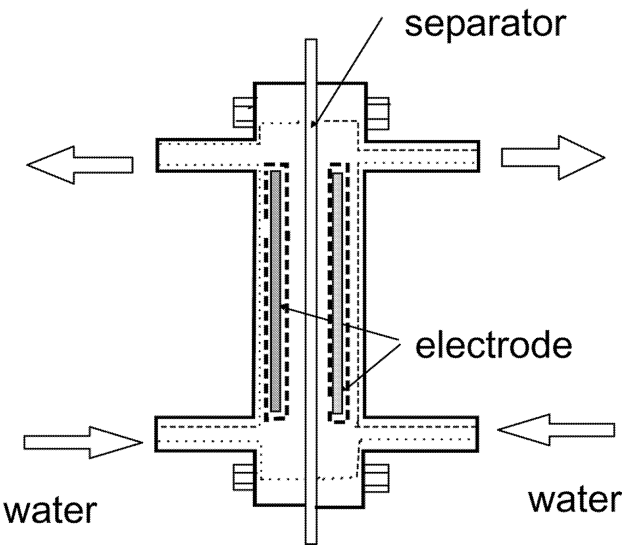

Fig. 1. Schematic of electrolytic cell.

height of the chamber housing the electrolytic cell was 10 cm. The volume of the chamber was 10 cm^3, and the effective surface area of the electrodes was 50 cm^2. The current density ranged from 0.02 to 1.60 A dm^{-2}. The electrodes used in the present study were titanium electroplated with platinum (Tanaka Kikinzoku Kogyo), titanium coated with sintered platinum (TDK Corp.), titanium coated with iridium–platinum alloy (TDK Corp.), and aged platinum. The aged platinum electrodes were prepared by aging a platinum plate in an argon atmosphere at 1500 °C for approximately 3 h. Nafion 117 (Du Pont Co.) was used as the separator. This electrolytic device is similar to a commercial Alkali–Ion–Water electrolyzer. The electrolytic solution was prepared by adding an electrolyte to purified water, and was then stored in a tank. The dissolved oxygen in the solution was purged by bubbling a pure gas (nitrogen, hydrogen or helium gas) through the solution for approximately 1 h. Two pumps were used, to supply solution to each chamber of the electrolytic cell at a fixed rate between 10 and 40 ml min^{-1}. Electrolysis was performed at a constant current controlled using a potentio-galvanostat (HA-105, Hokuto Denko Corp.).

The concentration of hydrogen in electrolyzed solution was determined as follows: A volume of a solution (50 ml) of 3 M (3 mol dm^{-3}) sulfuric acid and 0.01 M K_2CrO_4 was poured into a glass-stoppered flask of 300 ml capacity, to which 3 g of platinum powder was then added. The oxygen inside the flask was exchanged with nitrogen by bubbling nitrogen through the solution for 1 h. A sample of electrolyzed solution from the cathode chamber was then poured directly into the flask and stirred for approximately 30 min in order to oxidize the hydrogen with K_2CrO_4. A fraction of the solution was then titrated with an iron(II) solution in order to determine the amount of K_2CrO_4 that was consumed. The concentration of hydrogen was calculated based on the decrease in K_2CrO_4.

3. Results and discussion

The validity of the method used to determine the concentration of hydrogen was evaluated by constructing a calibration curve, as shown in Figure 2. The plots lie on a straight line, however, the error bars indicate a fairly low reproducibility and an error of approximately 5%. The saturated concentration of hydrogen obtained by bubbling hydrogen gas through water analyzed using this method gave 0.75 mM at 25 °C, which is in good agreement with the previously reported value [18]. The present analytical method was thus found to be adequately accurate for the purpose of the present study.

Figure 3 shows SEM images of the surfaces of the electrode materials. The roughness factors of the electrodes used in the present study are listed in Table 1. The roughness was estimated by measuring the adsorption wave for hydrogen [19]. As the roughness of the aged and electroplated electrodes was low, the actual current densities of these electrodes were higher than those of the other electrodes.

Figure 4 shows the effect of electrode material on the concentration of hydrogen in the solution. In this case, the current density was obtained by dividing the electrolytic current by the apparent surface area of the electrode (50 cm^2). The electrode materials were found to have a significant influence on the concentration. Electrodes of titanium coated with sintered platinum yielded the lowest hydrogen concentration, while electrodes of titanium electroplated with platinum and aged platinum resulted in higher concentrations. In all cases, the concentration of hydrogen was greater than the saturation concentration of hydrogen at 25 °C

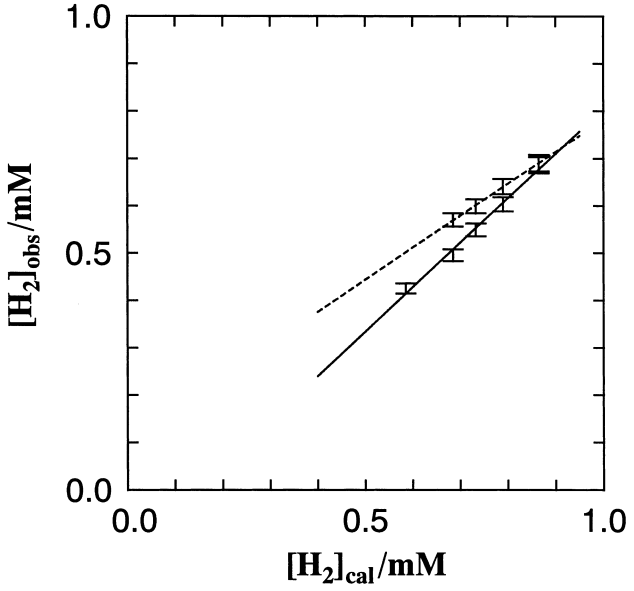

Fig. 2. Calibration curves of the concentration of hydrogen. $[H_2]_{cal}$ is concentration of hydrogen obtained from the reference [12] and $[H_2]_{obs}$ is concentration of hydrogen obtained using the present analysis method. Weight of platinum powder used in analysis: 5g (—); 3g (- - -).

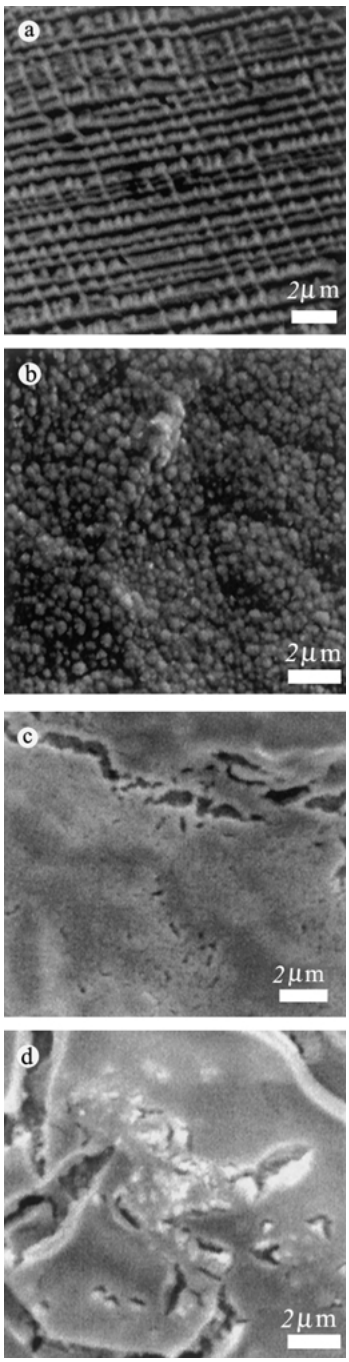

Fig. 3. SEM images of the surface of the electrodes materials. (a) aged platinum electrode; (b) titanium electrode electroplated with platinum; (c) titanium electrode coated with sintered platinum; (d) titanium electrode coated with iridium–platinum alloy.

(0.75 mM), indicating that the solutions were supersaturated with hydrogen. The mass of hydrogen produced by electrolysis was determined from the electrolysis current at fixed current efficiency. Most of the hydrogen produced at the electrode surface through the electrolysis of water diffuses into the bulk solution as dissolved hydrogen, and the remainder form bubble nuclei and subsequently escape the system as hydrogen bubbles grew from the nuclei. This phenomenon is expressed by the following equation:

Table 1. Roughness factor of electrode surface

Electrode materials	Roughness factor
Aged platinum	1.4
Titanium, electroplated with platinum	1.9
Titanium, coated with sintered platinum	21
Titanium, coated with iridium–platinum alloy	68

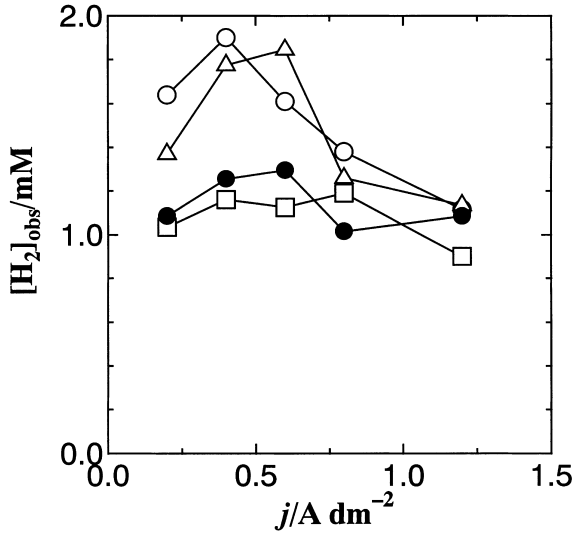

Fig. 4. Effect of electrode materials on the concentration of hydrogen in the solution containing 1.70 mM NaCl. Current density is the apparent current density. (○) aged platinum electrode; (△) titanium electrode electroplated with platinum; (□) titanium electrode coated with sintered platinum; (●) titanium electrode coated with iridium–platinum alloy.

$$\frac{kj}{2F} = KS\left(\frac{\partial C}{\partial x}\right)_{x=0} + f(C) \tag{1}$$

where j is current density, F is Faraday's constant, k is current efficiency, K is the average mass-transfer coefficient, C is the hydrogen concentration, S is the surface area of electrode, x is the distance from the electrode surface, and $f(C)$ represents the growth of hydrogen bubbles. The first term (diffusion term) on the right-hand side of Equation 1 expresses the diffusion of dissolved hydrogen away from the electrode surface into the bulk solution, and the second term (bubble growth term) represents the growth rate of hydrogen bubbles. The concentration of dissolved hydrogen in the electrolyzed solution is calculated according to the following equation:

$$(C_B - C_{B0})vS_C = KS\left(\frac{\partial C}{\partial x}\right)_{x=0} = SK_H \tag{2}$$

where C_B is the average bulk concentration of hydrogen at the exit of cell, C_{B0} is the initial bulk concentration of hydrogen, v is the average velocity of the solution, S_C is the cross-sectional area of the cathode chamber, and K_H

is the flux of hydrogen from the electrode surface to bulk solution, giving the concentration of dissolved hydrogen. If the solution does not contain bubbles, the laminar flow theory can be used for the electrolysis system [26]. The flux of hydrogen, K_H, is expressed as follows:

$$K_H = 0.646\frac{D}{L}\left(\frac{Lv\rho}{\mu}\right)^{1/2}\left(\frac{\mu}{\rho D}\right)^{1/3}(C_S - C_{B0}) \quad (3)$$

where D is the diffusion coefficient of hydrogen, L is the length of the electrode, μ is the viscosity of the solution, ρ is the density of the solution, and C_S is the concentration of hydrogen at the electrode surface. Introduction of Equations 2 and 3 to Equation 1 gives Equation 4.

$$\frac{kj}{2F} = 0.646\frac{D}{L}\left(\frac{Lv\rho}{\mu}\right)^{1/2}\left(\frac{\mu}{\rho D}\right)^{1/3}(C_S - C_{B0})S + f(C) \quad (4)$$

Janssen reported a similar mass-transfer coefficient for the diffusion term [21]. The presence of bubbles in a solution causes agitation, resulting in large K value [21]. For a given apparent current density, the actual current density on electrodes decreased in the order of aged platinum, platinum-electroplated titanium, titanium coated with sintered platinum, and titanium coated with iridium–platinum alloy. Higher current density results in an increase in the concentration of hydrogen at the surface of the electrode, as reported by Shibata [13] and Vogt [20, 22]. C_S decreases in the same order. Electrodes of titanium electroplated with platinum and aged platinum produced higher hydrogen concentrations than the other electrodes. High current density and high hydrogen concentration cannot be achieved using the sintered platinum or iridium–platinum alloy electrodes because the higher electrolysis current required to produce higher current densities elevated the temperature of the electrolyzed water. Therefore, the dissolution rate of hydrogen from the electrode surface to the bulk solution depends strongly on the concentration of hydrogen at the electrode surface.

For the electrodes of aged platinum and titanium electroplated with platinum, the hydrogen concentration–current density curve has a maximum at about 0.6 A dm^{-2}. Janssen and Barendrecht [23] reported a similar phenomena for oxygen evolution in alkaline aqueous solution. An increase in the current density to 0.6 A dm^{-2} results in an increase in hydrogen concentration at the electrode surface, in turn increasing the hydrogen content in bulk solution. Higher current density increases the supply of molecular hydrogen from the electrode surface, resulting in a higher bubble population density. An increased bubble population density causes the rate of absorption of dissolved hydrogen by bubbles to increase, resulting in a lower dissolved hydrogen concentration. This phenomenon is described by an increase in the bubble growth term.

The effect of solution flow rate on hydrogen concentration was then examined. The flow rate was controlled by varying the solution supply rate. As shown in Figure 5, the concentration of hydrogen decreased with increase in flow rate. The effect of concentration of sodium chloride on the hydrogen content can be seen in this figure. The concentration of hydrogen in a 1.57 mM (100 ppm) NaCl solution is lower than that in a 15.7 or 157 mM solution. Hence, an increase in the concentration of NaCl may lower the magnitude of the bubble growth term.

The relationship between the solution supply rate and the ratio of the observed hydrogen concentration to the theoretical, as obtained from the electrochemical equivalent calculated from the amount of charge passing through the electrolytic cell, is shown in Figure 6. The ratio corresponds to the current efficiency of hydrogen production in terms of the hydrogen concentration in the bulk solution. The ratio increased to 0.45 as a result of increasing the supply rate. An increase in flow rate results in an increase in the diffusion term in Equation 2 in the absence bubbles. The existence of bubbles not only makes the diffusion term larger but also decreases the thickness of the concentration boundary layer. Bubble nuclei are expected to form primarily within the boundary layer and grow in the middle region of the diffusion layer, as evidenced by the range of bubble diameters (4–120 μm) [24, 25]. A higher flow rate reduces the thickness of the boundary layer and results in an increase in the magnitude of the diffusion term in Equation 1. This, in turn, lowers the concentration at which bubbles grow and reduces the value of the bubble growth term in Equation 1. Then, the ratio of the

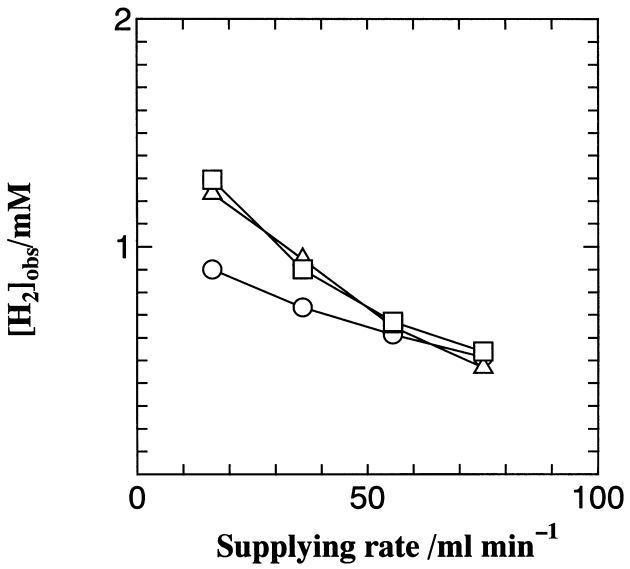

Fig. 5. Effect of the flow rate of the solution to the electrolytic cell on the concentration of hydrogen with titanium electrode electroplated with platinum at a current density of 0.6 A dm^{-2}. [NaCl] (mM): (○) 1.57; (△) 15.7; (□) 157.

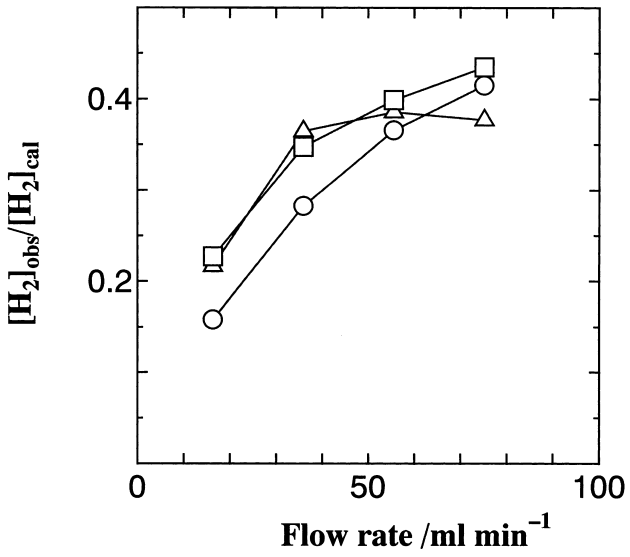

Fig. 6. The relation between the supply rate and the ratio of the observed to the theoretical hydrogen concentration. [NaCl] (mM): (○) 1.57; (△) 15.7; (□) 157.

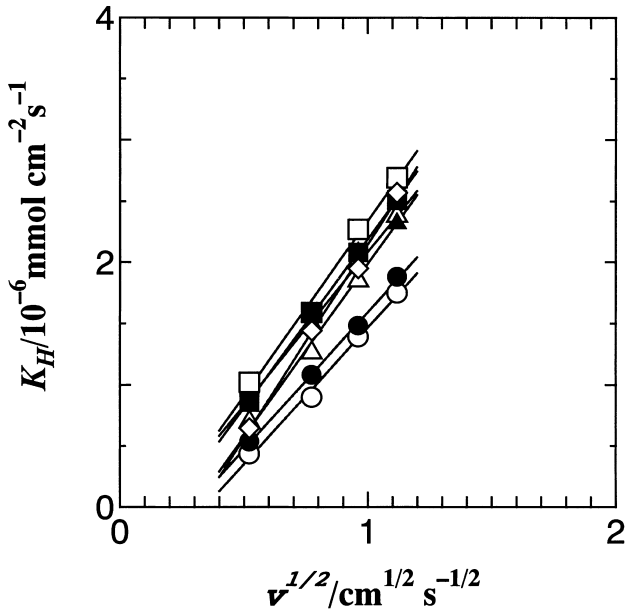

Fig. 7. Relation between the solution flow rate ($v^{1/2}$) and the hydrogen flux from the electrode surface to the bulk solution (K_H) in a solution of 0.010 M NaOH.

observed hydrogen concentration to the theoretical, increases with the flow rate.

Figure 7 shows the relationship between the solution flow rate ($v^{1/2}$) and the hydrogen flux from the electrode surface to the bulk solution (K_H). An increase in the current density can be seen to increase the slope of the line because the effect of bubble convection increases with current density. However, these plots fall on very straight lines, indicating that the flux (K_H) is more dependent on the solution flow rate than bubble convection. These observations are similar to those reported by Bendrich et al. [12]. They reported that the macroconvective mass transfer due to hydrodynamic flow along the electrode surface is the primary factor governing mass transfer in the case of low current density and high electrolyte velocity. In the present study, the primary factor was also observed to be hydrodynamic flow, described by Equation 2 for fixed current density.

Figure 8 shows the effect of flow rate on the concentration of hydrogen in a solution of 157 mM sodium chloride. These plots form a maximum at approximately 0.3 A dm^{-2}. The rate of dissolved hydrogen absorption by hydrogen bubbles increases with current density, giving a peak at current densities about 0.3 A dm^{-2}. The current density indicating the maximum value is independent of the flow rate. The profile of hydrogen concentration in the vicinity of electrode surface is expected to behave analogously, as evidenced by the similarity of the relationship between the diffusion and bubble growth terms.

The effect of cations on the dissolved hydrogen concentration is shown in Figure 9. The plots have a maximum at 0.25 A dm^{-2} for NaCl and KCl solutions, and a maximum at 0.5 A dm^{-2} for LiCl. Significant differences in the concentration of hydrogen were observed among these solutions. These differences may be due to the stability of the supersaturated hydrogen at the surface of the electrode solution, with stability decreasing in the order of lithium, sodium and then potassium ions.

Figure 10 shows the effect of the species of anion on the concentration of hydrogen. The concentration of hydrogen decreased in the order of chloride, nitrate and then sulfate ions, indicating that the rate of nucleation of hydrogen bubbles increases in the same order.

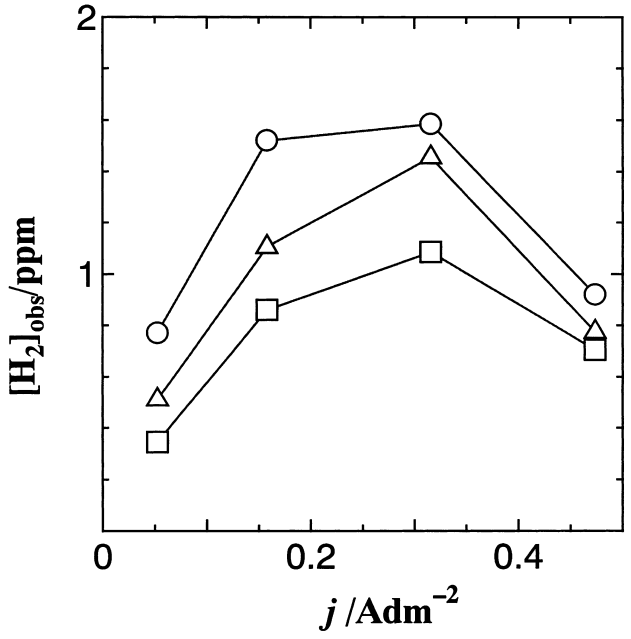

Fig. 8. Effect of the flow rate on the concentration of hydrogen in a solution containing 157 mM NaCl. Flow rate (ml min^{-1}): (○) 16.4; (△) 35.9; (□) 55.5.

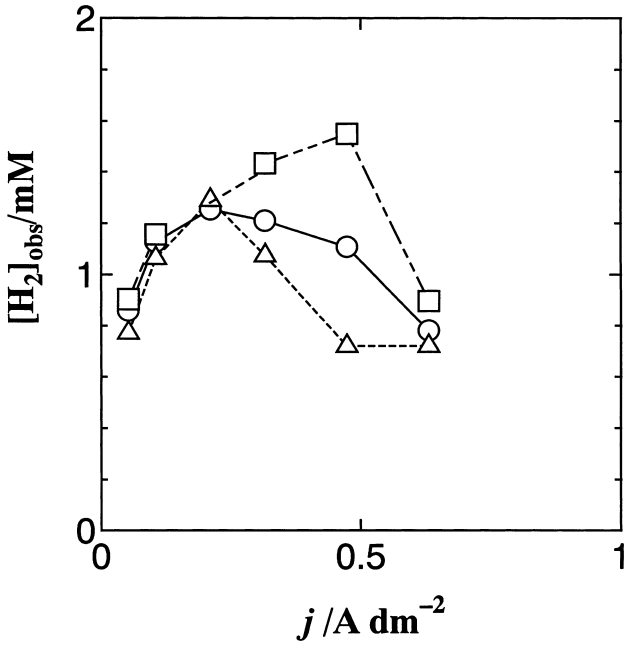

Fig. 9. Influence of cations on the concentration of hydrogen at a supply rate of 16.4 ml min^{-1}. (□) 1.57 mM LiCl; (○) 1.57 mM NaCl; (△) 1.57 mM KCl.

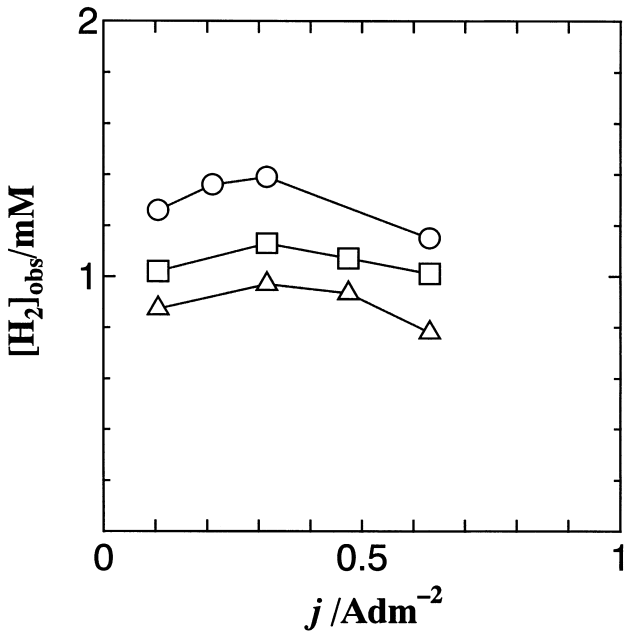

Fig. 10. Effect of the species of anion on the concentration of hydrogen at a supply rate 16.4 ml min^{-1}. (○) 1.57 mM NaCl; (△) 0.52 mM Na_2SO_4; (□) 1.57 mM $NaNO_3$.

The effect of the type of purge gas before electrolysis was also examined, with the finding that purge gas has no significant effect on the concentration of hydrogen at current densities over 0.03 A dm^{-2}.

5. Conclusion

The relationship between the hydrogen concentration in electrolyzed solution from a flow-type electrolytic cell and the electrolysis conditions was clarified. The change in hydrogen concentration as a function of current density gave an indication of the maximum concentration achievable in the solutions examined. The concentration of hydrogen was found to depend strongly on both the diffusion of hydrogen from the electrode surface to the bulk solution and bubble formation and bubble growth rates, as evidenced by the dependence of the maximum hydrogen concentration on current density and not the solution supply rate.

References

1. C.W.M.P. Sillen, E. Barendrecht, L.J.J. Janssen and S.J.D. van Strahlen, *Int. J. Hydrogen Energy* **7** (1982) 577.
2. V.G. Nefedov, *Russ. J. Electrochem.* **30** (1994) 1261.
3. V.G. Nefedov and V.M. Matveev, *Russ. J. Electrochem.* **30** (1994) 1264.
4. Y. Chogutte, H. Menard and L. Brossard, *Int. J. Hydrogen Energy* **15** (1990) 21.
5. G. Krenpa, B. Hakansson and P. Ekudunce, *Electrochim. Acta* **33** (1988) 1351.
6. A. Iwasaki, H. Kaneko, Y. Abe and M. Kamimoto, *Electrochim. Acta* **43** (1988) 509.
7. B.E. El-Anadouli, M.M. Khader, M.M. Saleh and B.G. Ateya, *J. Applied Electrochem.* **21** (1991) 166.
8. J.Y. Huot, M.L. Trudeau and R. Schulz, *J. Electrochem. Soc.* **138** (1991) 1316.
9. P. Ekdunge, K. Juttner, G. Kreysa, T. Kessler, M. Ebert and W.J. Lorenz, *J. Electrochem. Soc.* **138** (1991) 2260.
10. H. Wendt, H. Hofmann and V. Plzak, *Mat. Chem. Phys.* **22** (1989) 29.
11. H. Wendt and H. Hofmann, *J. Appl. Chem.* **19** (1989) 605.
12. G. Bendrich, W. Seiler and H. Vogt, *Int. J. Heat Mass Transfer* **29** (1986) 1741.
13. S. Shibata, *Bull. Chem. Soc. Japan* **36** (1963) 53.
14. S. Shibata, *Electrochim. Acta* **23** (1978) 619.
15. K. Miyashita, M. Yasuda, T. Ota and T. Suzuki, *Biosci. Biotechnol. Biochem.* **63** (1999) 421.
16. S. Shirahata, S. Kabayama, M. Miura, K. Kusumoto and Y. Katakura, *Biochem. Biophys. Res. Commu.* **234** (1997) 269.
17. S. Suzuki, M. Nishina, T. Kuramochi, Y. Yamakawa, K. Yabe and M. Suzuki, *Med. Biol.* **131** (1995) 281.
18. C.L. Young, Ed., *IUPAC Solubility Data Series*, Vol. 5/6, Hydrogen and Deuterium, (Pergamon Press, Oxford, England, 1981).
19. R. Wood, In A.J. Bard (ed.), *Electroanalytical Chemistry*, Vol. 9, (Marcel Dekker, New York, 1976).
20. H. Vogt, *Electrochim. Acta* **32** (1987) 633.
21. L.J.J. Janssen, *J. Appl. Electrochem.* **17** (1987) 1177.
22. H. Vogt, *Electrochim. Acta* **34** (1989) 1429.
23. L.J.J. Janssen and E. Barendrecht, *Electrochim. Acta* **29** (1984) 1207.
24. J.P. Glas and J.W. Westwater, *Int. J. Heat Mass Transfer* **7** (1964) 1427.
25. P. Boissonneau and P. Byrne, *J. Appl. Electrochem.* **30** (2000) 767.
26. E.L. Cussler, Diffusion Mass Transfer in Fluid Systems (Cambridge University Press, England, 1997).